NACA

RESEARCH MEMORANDUM

AERODYNAMIC STUDY OF A WING-FUSELAGE COMBINATION

EMPLOYING A WING SWEPT BACK 63°.- AERODYNAMIC

CHARACTERISTICS IN SIDESLIP OF A LARGE-SCALE

MODEL HAVING A 63° SWEPT-BACK

VERTICAL TAIL

By Gerald M. McCormack

Ames Aeronautical Laboratory
Moffett Field, Calif.

NATIONAL ADVISORY COMMITTEE
FOR AERONAUTICS

WASHINGTON
October 7, 1949

NATIONAL ADVISORY COMMITTEE FOR AERONAUTICS

RESEARCH MEMORANDUM

AERODYNAMIC STUDY OF A WING-FUSELAGE COMBINATION EMPLOYING A WING

SWEPT BACK 63°.— AERODYNAMIC CHARACTERISTICS IN SIDESLIP OF A

LARGE-SCALE MODEL HAVING A 63° SWEPT-BACK VERTICAL TAIL

By Gerald M. McCormack

SUMMARY

An investigation has been conducted to determine the effects of a vertical tail having the leading edge swept back 63° on the aerodynamic characteristics of a wing—fuselage combination employing a wing with the leading edge swept back 63°. The aerodynamic characteristics in sideslip with and without the vertical tail are presented. Included also are the rudder effectiveness and the rudder hinge—moment characteristics.

At angles of attack from 0° to 12°, the effectiveness of the vertical tail was maintained to an angle of sideslip of 25° (the highest tested). At an angle of attack of 21°, however, effectiveness was maintained only to an angle of sideslip of about 7°; beyond 7° the directional stability was irregular.

The rudder was effective throughout the range of angles of attack and of angles of sideslip tested. At an angle of attack of 21°, however, at angles of sideslip greater than about 9°, rudder effectiveness was considerably less than at the lower angles.

The experimental characteristics are compared with characteristics computed theoretically in order to provide a basis for estimating the effects of geometric changes of the vertical tail.

INTRODUCTION

A possible aircraft configuration suitable for flight at Mach numbers up to about 1.5 is undergoing study in the research facilities of the Ames Aeronautical Laboratory to provide information relative to its aerodynamic behavior over a range of Reynolds numbers and Mach numbers. The configuration is based on the principles outlined in reference 1 which indicate that aircraft employing highly swept slender wings should be capable of relatively efficient flight ($L/D \approx 10$) at moderate supersonic speeds. The

model used in this study incorporates a wing of 63° leading—edge sweep—back, aspect ratio 3.5, and taper ratio 0.25, in combination with a fine—ness ratio 12.5 fuselage.

The aerodynamic characteristics of the wing and wing—body combina—tion at various Reynolds numbers and at subsonic and supersonic Mach numbers, and the effects of various modifications, controls, and high lift devices have been reported in references 2 to 8.

It was shown in reference 2 that at low speeds the wing alone pos—sessed neutral directional stability. The wing—fuselage combination was found to have a large amount of instability and it is anticipated that the same situation will also exist at high speeds. Insufficient data exist to allow a rational determination of the amount of directional stability required at either low or high speeds for the subject configu—ration. To provide information as to the effectiveness of a vertical tail on such a configuration, however, a vertical tail designed to provide an average amount of stability according to present standards was incorporated on the large—scale model described in reference 2. The tail had the same sweep (63° of the leading edge), aspect ratio (1.75), and taper ratio (0.25) as a semispan of the wing.

This report presents the aerodynamic characteristics in sideslip of the large—scale wing—fuselage combination with and without the vertical tail as determined in the Ames 40— by 80—foot wind tunnel. Included also are the rudder effectiveness and rudder hinge—moment characteristics.

NOTATION

The data are presented in the form of standard NACA coefficients and symbols as defined in figure 1 and the following tabulation. All forces and moments were computed about the stability axes with the origin located in the plane of symmetry of the model at the same vertical and fore—and—aft location as the quarter—chord point of the mean aerodynamic chord. (The stability axes are a system of axes in which the normal (lift) axis lies in the plane of symmetry and is perpendicular to the relative wind; the longitudinal (drag) axis lies in the plane of symmetry and is perpendicular to the normal axis; and the lateral axis is perpen—dicular to the plane of symmetry.)

C_L lift coefficient $\left(\dfrac{\text{lift}}{qS}\right)$

C_D drag coefficient $\left(\dfrac{\text{drag}}{qS}\right)$

C_m pitching—moment coefficient $\left(\dfrac{\text{pitching moment}}{qS\bar{c}}\right)$

C_l rolling—moment coefficient $\left(\dfrac{\text{rolling moment}}{qSb}\right)$

C_n yawing–moment coefficient $\left(\dfrac{\text{yawing moment}}{qSb}\right)$

C_Y side–force coefficient $\left(\dfrac{\text{side force}}{qS}\right)$

C_{l_β} rate of change of rolling–moment coefficient with angle of sideslip, per degree

C_{n_β} rate of change of yawing–moment coefficient with angle of sideslip, per degree

C_{Y_β} rate of change of side–force coefficient with angle of side-slip, per degree

$\Delta C_{n_{\beta_t}}$ increment of the rate of change of yawing–moment coefficient with angle of sideslip due to adding the vertical tail, per degree

$C_{n_{\delta_r}}$ rate of change of yawing–moment coefficient with angle of rudder deflection, per degree

$C_{h_{\delta_r}}$ rate of change of rudder hinge–moment coefficient with angle of rudder deflection, per degree

c_{h_δ} value in two–dimensional flow of the rate of change of flap hinge–moment coefficient with angle of flap deflection, per degree

$C_{h_{\alpha_t}}$ rate of change of rudder hinge–moment coefficient with angle of attack of vertical tail, per degree

c_{h_α} value in two–dimensional flow of the rate of change of flap hinge–moment coefficient with angle of attack of airfoil, per degree

$dC_N/d\delta_r$ rate of change of the vertical–tail normal–force coefficient with angle of rudder deflection, per degree

$(dC_N/d\alpha)_t$ rate of change of the vertical–tail normal–force coefficient with angle of attack of the vertical tail, per degree

L/D ratio of lift to drag

α_δ relative rudder effectiveness $\left[\dfrac{dC_N/d\delta_r}{(dC_N/d\alpha)_t}\right]$

α angle of attack, degrees

β angle of sideslip, degrees

CONFIDENTIAL

Γ_e effective dihedral, degrees

δ_r rudder angle, measured in a plane perpendicular to the hinge line, degrees

$\Lambda_{c/4}$ angle of sweepback of quarter-chord line, degrees

σ angle of sidewash, degrees
(Negative when it increases the angle of attack of the vertical tail.)

$d\sigma/d\beta$ rate of change of angle of sidewash with angle of sideslip

q dynamic pressure, pounds per square foot

q_t/q ratio of the effective dynamic pressure at the vertical tail to the free-stream dynamic pressure

A_t aspect ratio of swept-back vertical tail

S wing area, square feet

S_t vertical-tail area, square feet

b wing span measured perpendicular to the plane of symmetry, feet

c local chord, feet

$\bar{c}$ wing mean aerodynamic chord $\left(\dfrac{\int_0^{b/2} c^2 \, dy}{\int_0^{b/2} c \, dy} \right)$, feet

l_t distance from the quarter-chord point of the mean aerodynamic chord of the wing to the rudder hinge line at the mean aerodynamic chord of the vertical tail

y spanwise coordinate perpendicular to plane of symmetry, feet

MODEL

The wing-fuselage combination was the same as that used in reference 2. The wing had the leading edge swept back 63°, an aspect ratio of 3.5, a taper ratio of 0.25, no twist, and no dihedral. It had an NACA 64A006 section in a streamwise direction. The fuselage had a fineness ratio of 12.5, an elliptical lengthwise section, and a circular cross section. The wing was mounted on the fuselage center line with zero incidence.

CONFIDENTIAL

The vertical tail used had the same plan form[1] as a half—span of the wing: the leading edge swept back 63°, an aspect ratio of 1.75, a taper ratio of 0.25, and an NACA 64A006 section in a streamwise direction. Certain geometric characteristics of the tail pertinent to computations are given in the following tabulation:

Item	Symbol	Value
Relative tail area	S_t/S	0.168
Relative tail length	$l_t/\bar{c}$	2.41
Relative tail volume	$S_t \times l_t / S \times \bar{c}$	0.404

The vertical tail was equipped with a rudder having a ratio of flap chord to total chord of 0.25. The rudder had a minimum of balance, the nose of the rudder being an arc with a radius equal to half the airfoil thickness at the hinge line. The gap between rudder and fin was 1 percent of the local chord perpendicular to the leading edge and was unsealed. The rudder was equipped with a strain gage to provide hinge—moment data.

Photographs of the model mounted in the wind tunnel are shown in figure 2. The dimensions of the model are shown in figure 3. Based on a wing loading of 50 pounds per square foot and a design weight of 40,000 pounds, the model tested in the Ames 40— by 80—foot wind tunnel was about half scale.

TESTS

Six—component force data were obtained for the model with tail off, with tail on and rudder undeflected, and with tail on and rudder deflected to various set angles. Rudder hinge—moment data were also obtained. The data were obtained by varying the angle of sideslip while maintaining a constant angle of attack. All data were obtained at a tunnel speed of approximately 100 miles per hour, corresponding to a Reynolds number of 8.0×10^6 based on the mean—aerodynamic—chord length of 8.639 feet.

Standard tunnel—wall corrections for a straight wing of the same area and span as the swept—back wing have been applied to angle—of—attack and drag—coefficient data. This procedure was followed, since a brief analysis indicated that tunnel—wall corrections were approximately the same for straight and swept wings of the size under consideration. The corrections applied are as follows:

---

[1]The tail area and span used herein were measured to the center line of the fuselage.

$$\Delta\alpha = 0.48 \ c_L$$

$$\Delta c_D = 0.0084 \ c_L{}^2$$

No corrections have been applied for the drag and interference of the struts. With the exception of the effects on the drag results, these corrections are felt to be negligible. The effect on drag is of the order of $\Delta c_D = 0.008$ at zero lift, but is not known with sufficient accuracy to warrant application.

RESULTS

The aerodynamic characteristics of the model with the tail off are shown in figure 4; the characteristics with the tail on and the rudder undeflected are shown in figure 5. At angles of attack from 0° to 12°, the effectiveness of the vertical tail (fig. 5) was maintained to an angle of sideslip of 25° (the highest tested). At an angle of attack of 21°, however, effectiveness was maintained only to an angle of sideslip of 7°; beyond 7° the directional stability was irregular. This is the same attitude at which the directional stability of the model with tail off (fig. 4) became irregular.

The variations with angle of attack of the directional-stability derivative C_{n_β} and of the effective-dihedral derivative C_{l_β} are shown in figure 6. The values of the derivatives shown in figure 6 are the values at zero sideslip angle. Above an angle of attack of 7° with the vertical tail on, the value of C_{n_β} gradually decreased until at an angle of attack of 21° it was about 70 percent of the value at low angles of attack. The vertical tail increased the value of C_{l_β} up to an angle of attack of approximately 9°. Beyond 9°, the value of C_{l_β} was lower with the tail on than with the tail off.

The yawing-moment and the rudder hinge-moment characteristics of the model with the tail on and the rudder deflected to various angles are shown in figures 7 and 8. The rudder was effective throughout the range of angles of attack and angles of sideslip tested. At an angle of attack of 21°, however, at angles of sideslip greater than about 9°, rudder effectiveness was considerably less than at the lower angles.

A summary of various aerodynamic characteristics[2] of the model with and without the vertical tail is given in the following tabulation:

---

[2]Except for $C_{l_{\beta_{max}}}$, these are average values at zero angle of attack, zero angle of sideslip, and, where pertinent, zero angle of rudder deflection.

Parameter	Value	
	Tail off	Tail on
C_{n_β}	-0.0012	0.0025
$C_{l_{\beta_{max}}}$	-.0033($\Gamma_e \simeq 15°$)	-.0026($\Gamma_e \simeq 12°$)
$dC_{l_\beta}/d\alpha$	-.00022	-.00027
C_{Y_β}	-.0008	-.0061
$C_{n_{\delta_r}}$	- - -	-.0011
$C_{h_{\delta_r}}$	- - -	-.0029
$C_{h_{\alpha_t}}$	- - -	-.0006

DISCUSSION

In order to enable some generalizations to be made of the characteristics of the swept-back vertical tail and provide a basis for estimating the effects of geometric changes of the tail surface, various characteristics of the vertical tail have been computed theoretically. In the following discussion, the various factors involved in the theoretical computations are discussed and the experimental and theoretical results are compared.

Directional Stability

The stabilizing effect of a vertical tail can be estimated by use of the following equation:

$$\Delta C_{n_{\beta_t}} = \left(\frac{dC_N}{d\alpha}\right)_t \times \left(1 + \frac{d\sigma}{d\beta}\right) \times \frac{q_t}{q} \times \frac{S_t}{S} \times \frac{l_t}{b} \tag{1}$$

A way of estimating the tail normal-force-curve slope $\left(\frac{dC_N}{d\alpha}\right)_t$ is by the use of the data in reference 9. These data, however, are for complete wings and, therefore, in applying these data, the end-plate effect of the fuselage is assumed to be total. This procedure necessarily will require a correction to account for the

imperfect end–plate effect of the fuselage.[3] At the present time, how-
ever, the end–plate effect of a fuselage on a vertical tail has not been
determined either theoretically or experimentally; hence, no such correc-
tion will be used. Accordingly, the value of normal–force–curve slope of
the swept–back tail of 0.041 per degree, obtained from reference 9 assum-
ing the fuselage to exert a total end–plate effect, will be used. (This
compares to the lift–curve slope of 0.042 per degree measured for the full-
span wing of the same plan form, reference 2.)

In order to evaluate the sidewash term $1 + \frac{d\sigma}{d\beta}$ and the effective
dynamic pressure term $\frac{q_t}{q}$ for equation (1), surveys were made of the
air flow in the region of the tail. The integrated value of the average
dynamic pressure $\frac{q_t}{q}$ was found to be very nearly equal to 0.9. This is
consistent with unswept configurations. No consistent deviation from
zero sidewash was measurable, that is, $\frac{d\sigma}{d\beta} = 0$.

By the use of the above values of $\left(\frac{dC_N}{d\alpha}\right)_t$, $\frac{d\sigma}{d\beta}$, and $\frac{q_t}{q}$, together
with the dimensional characteristics of the model, the stabilizing effect
of the vertical tail (equation (1)) was computed which can be compared
with the experimental result:

Theoretical $\Delta C_{n_{\beta_t}} = 0.0048$

Experimental $\Delta C_{n_{\beta_t}} = 0.0037$

Rudder Effectiveness

The rudder effectiveness can be estimated from the following
equation:

$$C_{n_{\delta_r}} = -\left(\frac{dC_N}{d\alpha}\right)_t \times \alpha_\delta \times \frac{q_t}{q} \times \frac{S_t}{S} \times \frac{l_t}{b} \qquad . \quad (2)$$

The same value of the tail normal–force–curve slope will be used,
0.041 per degree (reference 9, assuming a total end–plate effect of the
fuselage).

The flap–effectiveness parameter α_δ can be estimated by applying
a correction for the effect of sweep to the value of α_δ of an equiva-
lent unswept, flapped airfoil. The parameter α_δ for an equivalent

[3]This is in contrast to the usual design procedure for unswept tails in
which the starting point is zero end–plate effect, a correction fac-
tor then being applied to increase the aspect ratio to account for the
end–plate effect of the horizontal tail.

unswept airfoil $\left(\dfrac{\text{unswept rudder chord}}{\text{unswept fin chord}} = 0.318\right)$ was estimated to have a value of about 0.47. It can be shown that, in accordance with the concepts of simple sweep theory (reference 10), α_δ should decrease in proportion to $\cos \Lambda_{c/4}$ if the airfoil is swept back and flap deflection is measured in a plane perpendicular to the hinge line. Applying this correction will give a value of α_δ of 0.23 for the swept-back vertical tail.

The rudder effectiveness (equation (2)) computed by using the above values agreed with the experimental value:

$$\text{Theoretical} \quad C_{n_{\delta_r}} = -0.0011$$

$$\text{Experimental} \quad C_{n_{\delta_r}} = -0.0011$$

Rudder Hinge Moments

An estimation of the rudder-hinge-moment parameters can be obtained by applying the concepts of simple sweep theory to two-dimensional characteristics. Thus, when the correction for aspect ratio[4] is included, the equations for the hinge-moment parameters can be written as follows:

$$C_{h_{\alpha_t}} = c_{h_\alpha} \times \cos \Lambda_{c/4} \times \frac{2A_t}{2A_t+2} \tag{3}$$

$$C_{h_{\delta_r}} = c_{h_\delta} \times \cos^2 \Lambda_{c/4} - c_{h_\alpha} \times \alpha_\delta \times \cos^2 \Lambda_{c/4} \times \frac{2A_t}{2A_t+2} \tag{4}$$

The two-dimensional values of c_{h_α} and c_{h_δ} have been estimated to be -0.0070 and -0.0125, respectively. By the use of these values in equations (3) and (4), $C_{h_{\alpha_t}}$ and $C_{h_{\delta_r}}$ were computed and can be compared to the experimental results:

	$C_{h_{\alpha_t}}$	$C_{h_{\delta_r}}$
Theoretical	-0.0022	-0.0026
Experimental	-.0006	-.0029

---

[4]Similar to the prediction of $\Delta C_{n_{\beta_t}}$, the aspect ratio of the tail, assuming a complete end-plate effect of the fuselage, will be used. This is twice the aspect ratio of the semispan tail.

CONCLUDING REMARKS

An investigation has been conducted to determine the effects of a vertical tail with the leading edge swept back 63° on the aerodynamic characteristics of a wing-fuselage combination employing a wing with 63° of sweep at the leading edge.

At angles of attack from 0° to 12°, the effectiveness of the vertical tail was maintained to an angle of sideslip of 25° (the highest tested). At an angle of attack of 21°, however, effectiveness was maintained only to an angle of sideslip of about 7°; beyond 7° the directional stability was irregular.

The rudder was effective throughout the range of angles of attack and of angles of sideslip tested. At an angle of attack of 21°, however, at angles of sideslip greater than about 9°, the rudder effectiveness was considerably less than at the lower angles.

Ames Aeronautical Laboratory,
    National Advisory Committee for Aeronautics,
        Moffett Field, Calif.

REFERENCES

1. Jones, Robert T.: Estimated Lift-Drag Ratios at Supersonic Speed. NACA TN 1350, 1947.

2. McCormack, Gerald M., and Walling, Walter C.: Aerodynamic Study of a Wing-Fuselage Combination Employing a Wing Swept Back 63°.— Investigation of a Large-Scale Model at Low Speed. NACA RM A8D02, 1949.

3. Reynolds, Robert M., and Smith, Donald W.: Aerodynamic Study of a Wing-Fuselage Combination Employing a Wing Swept Back 63°.— Subsonic Mach and Reynolds Number Effects on the Characteristics of the Wing and on the Effectiveness of an Elevon. NACA RM A8D20, 1948.

4. Madden, Robert T.: Aerodynamic Study of a Wing-Fuselage Combination Employing a Wing Swept Back 63°.— Characteristics at a Mach Number of 1.53 Including Effect of Small Variations of Sweep. NACA RM A8J04, 1949.

5. Madden, Robert T.: Aerodynamic Study of a Wing-Fuselage Combination Employing a Wing Swept Back 63°.— Investigation at a Mach Number of 1.53 to Determine the Effects of Cambering and Twisting the Wing for a Uniform Load at a Lift Coefficient of 0.25. NACA RM A9C07, 1949.

6. Hopkins, Edward J.: Aerodynamic Study of a Wing–Fuselage Combination Employing a Wing Swept Back 63°.— Effects of Split Flaps, Elevons, and Leading–Edge Devices at Low Speed. NACA RM A9C21, 1949.

7. Jones, Lloyd J.. and Demele, Fred A.: Aerodynamic Study of a Wing–Fuselage Combination Employing a Wing Swept Back 63°.— Characteristics Throughout the Subsonic Speed Range with the Wing Cambered and Twisted for a Uniform Load at a Lift Coefficient of 0.25. NACA RM A9D25, 1949.

8. Mas, Newton: Aerodynamic Study of a Wing–Fuselage Combination Employing a Wing Swept Back 63°.— Characteristics for Symmetrical Wing Sections at High Subsonic and Moderate Supersonic Mach Numbers. NACA RM A9E09, 1949.

9. DeYoung, John: Theoretical Additional Span Loading Characteristics of Wings With Arbitrary Sweep, Aspect Ratio, and Taper Ratio. NACA TN 1491, 1947.

10. Betz, A.: Applied Airfoil Theory. Unsymmetrical and Non–Steady Types of Motion. Vol. IV of Aerodynamic Theory, div. J, ch. IV, sec. 4, W. F. Durand, ed., Julius Springer (Berlin), 1935, pp. 94–107.
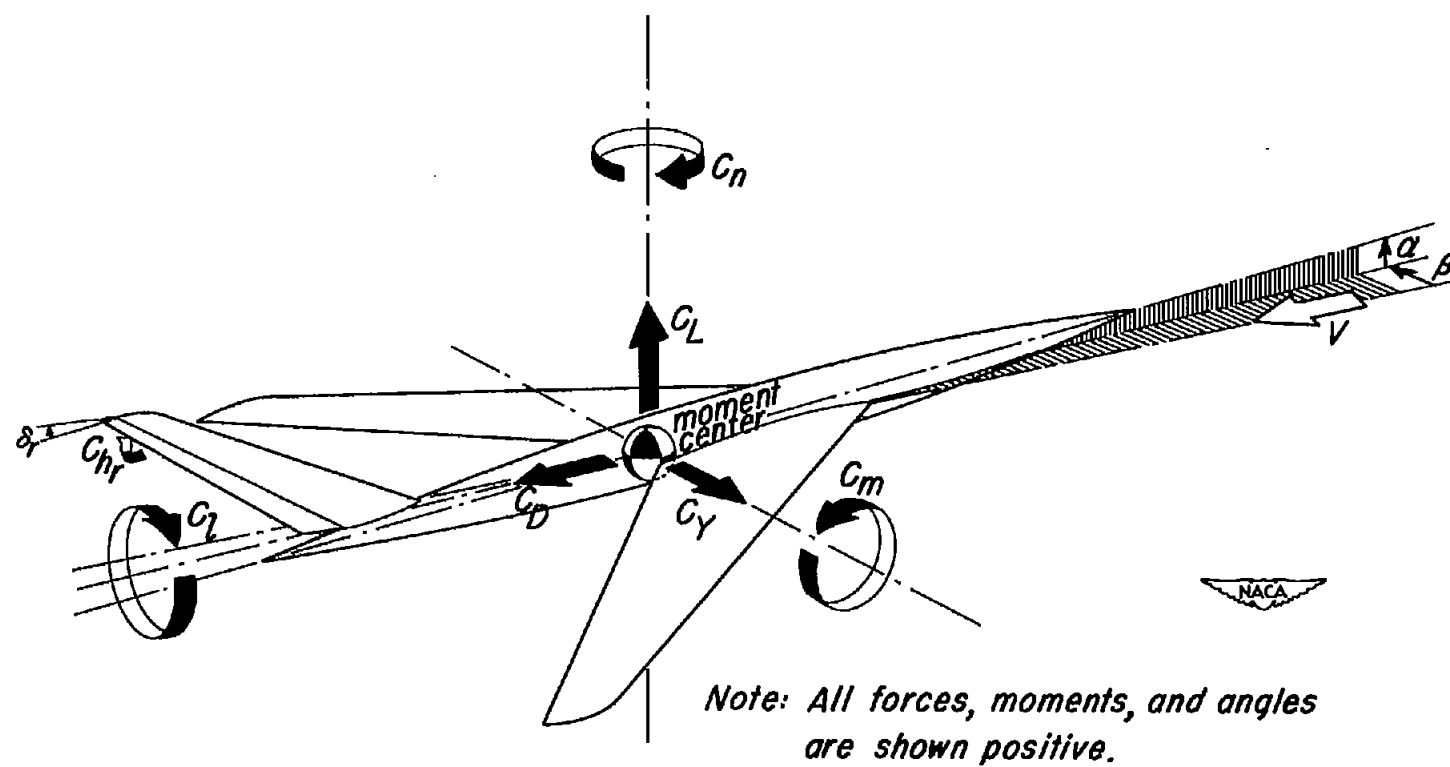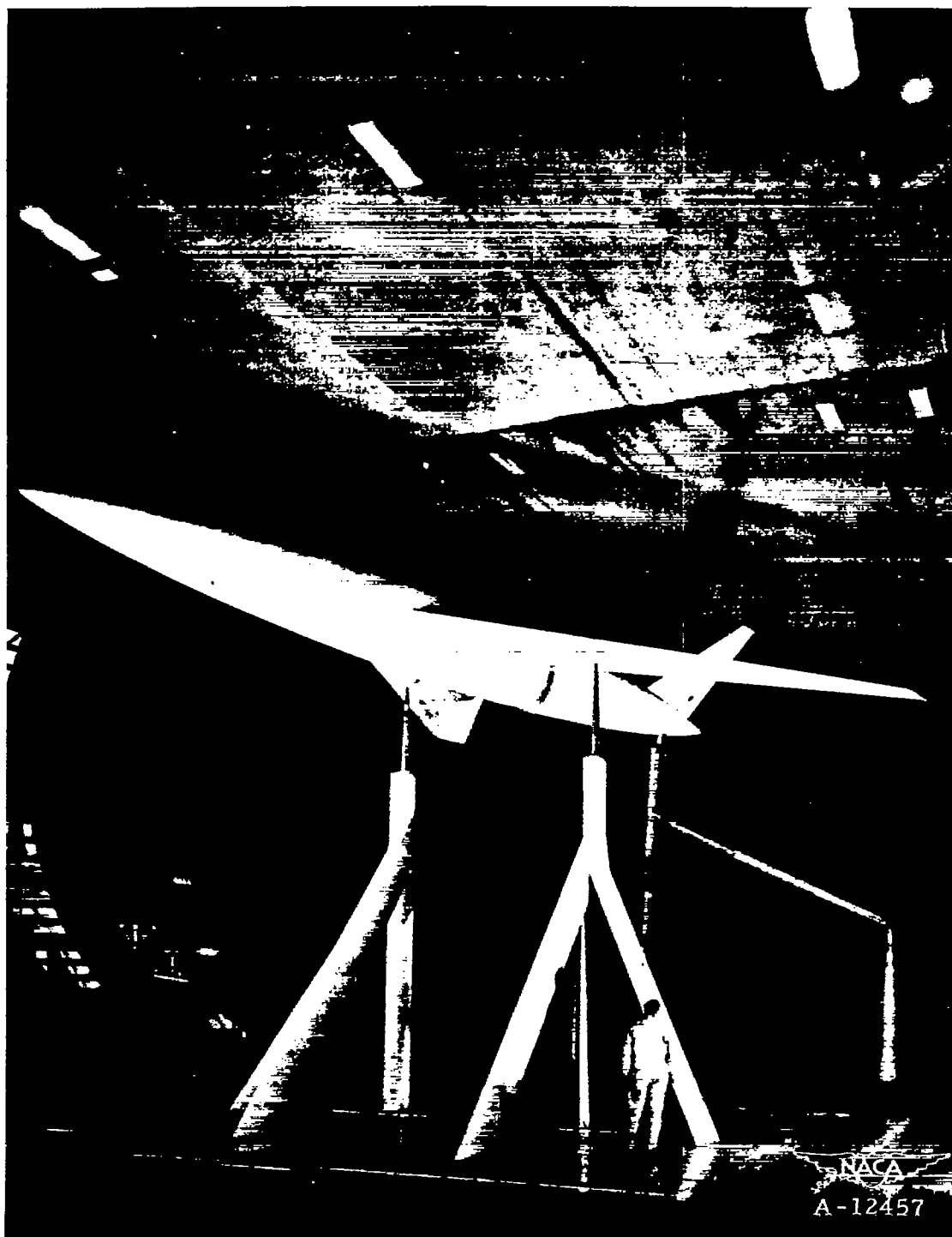
Note: All forces, moments, and angles are shown positive.

Figure I.–Standard NACA sign convention.

(a) Three—quarter front view.

Figure 2.— The 63° swept—back wing—fuselage combination with 63°
swept—back vertical tail.

(b) Close-up side view.

Figure 2.— Concluded.

Moment center
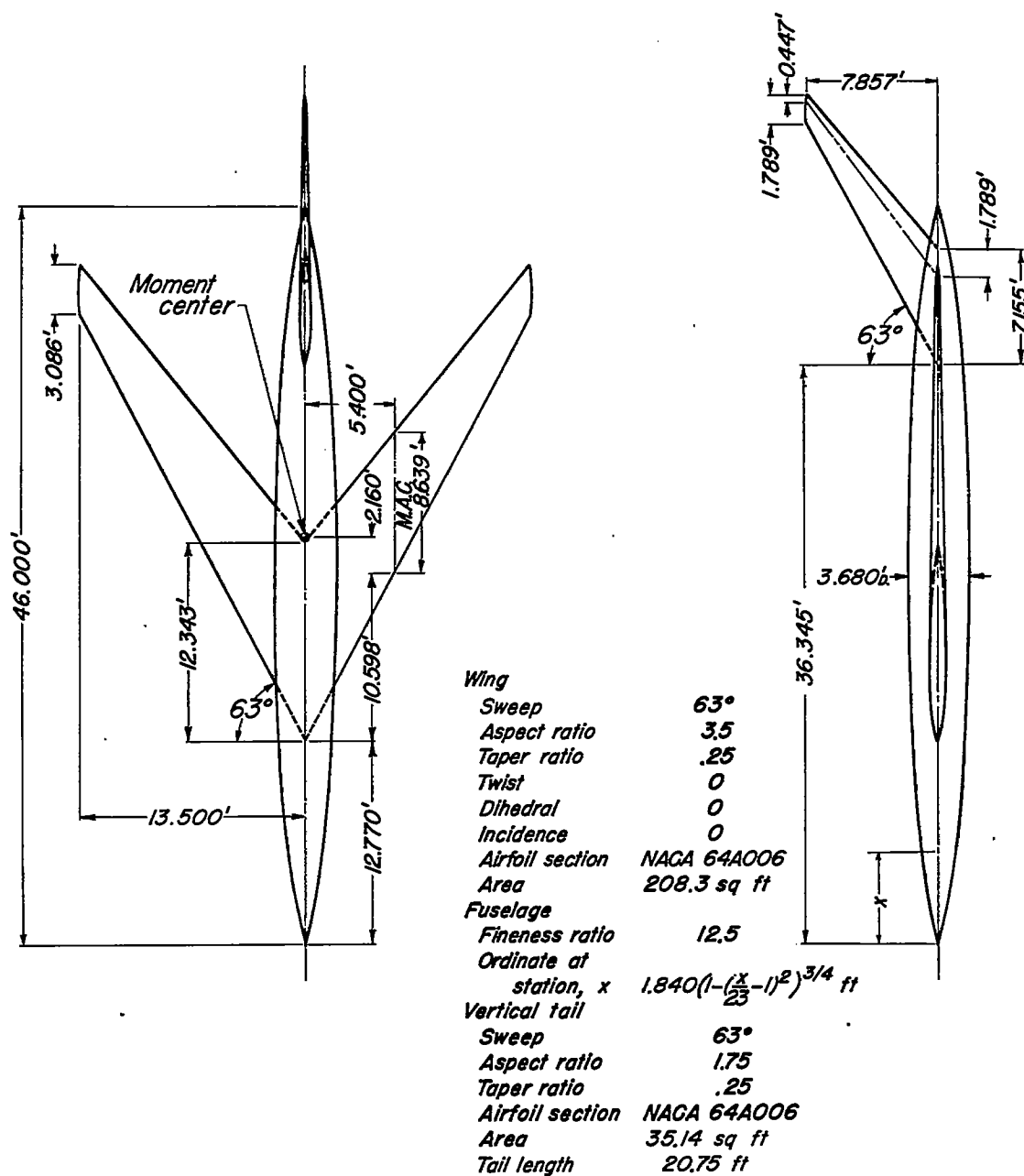
3.086'

46.000'

5.400'

M.A.C. .8639'

2.160'

12.343'

63°

10.598'

13.500'

12.770'

0.447'

7.857'

1.789'

1.789'

7.155'

63°

3.680'

36.345'

x

Wing
  Sweep   63°
  Aspect ratio   3.5
  Taper ratio   .25
  Twist   0
  Dihedral   0
  Incidence   0
  Airfoil section   NACA 64A006
  Area   208.3 sq ft
Fuselage
  Fineness ratio   12.5
  Ordinate at
    station, x $1.840\left(1-\left(\frac{x}{23}-1\right)^2\right)^{3/4}$ ft
Vertical tail
  Sweep   63°
  Aspect ratio   1.75
  Taper ratio   .25
  Airfoil section   NACA 64A006
  Area   35.14 sq ft
  Tail length   20.75 ft

Figure 3. — Geometric characteristics of 63° swept-back wing-fuselage combination with 63° swept-back vertical tail.
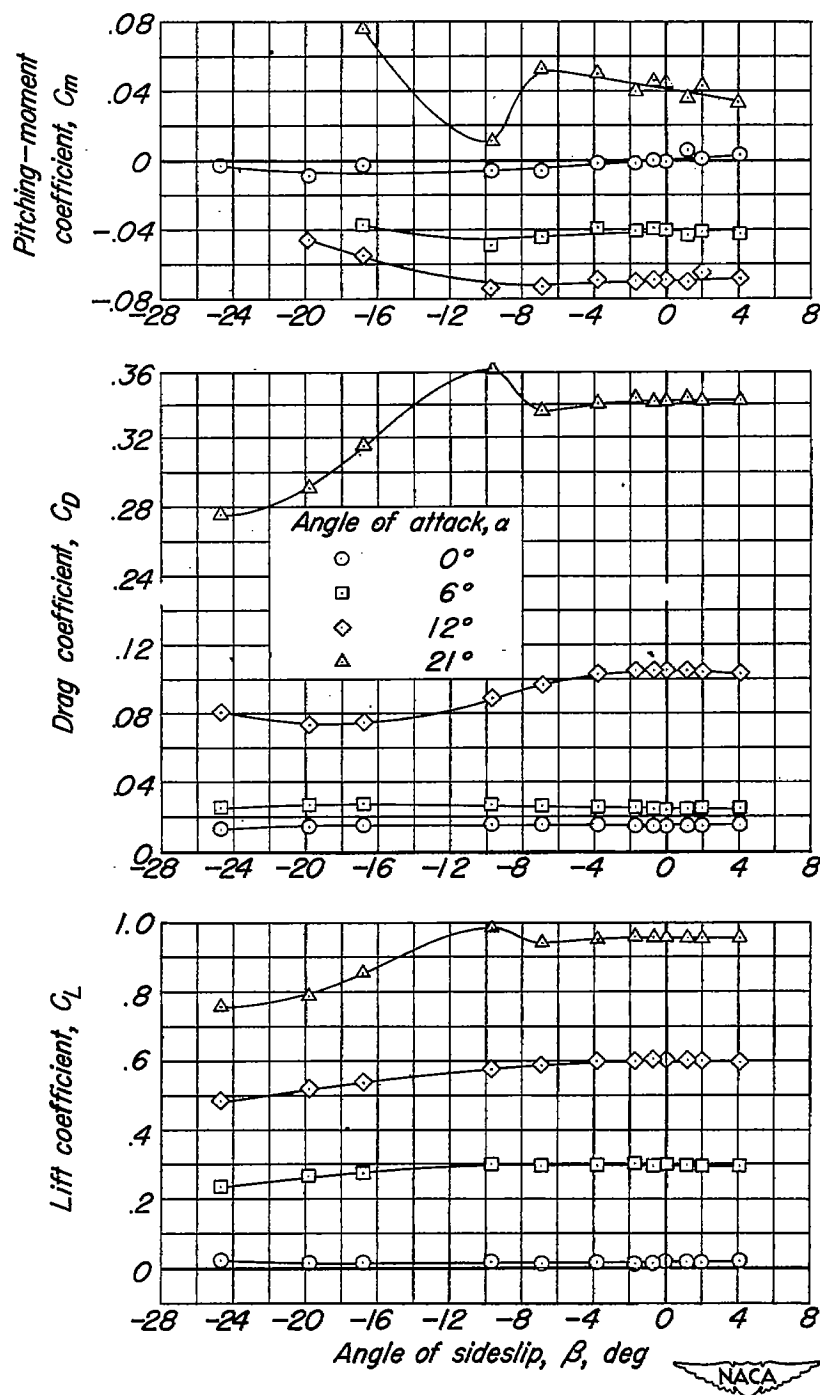
(a) C_m, C_D, C_L vs β.

Figure 4 . — Aerodynamic characteristics at several angles of attack of the 63° swept-back wing with fuselage. Vertical tail off.
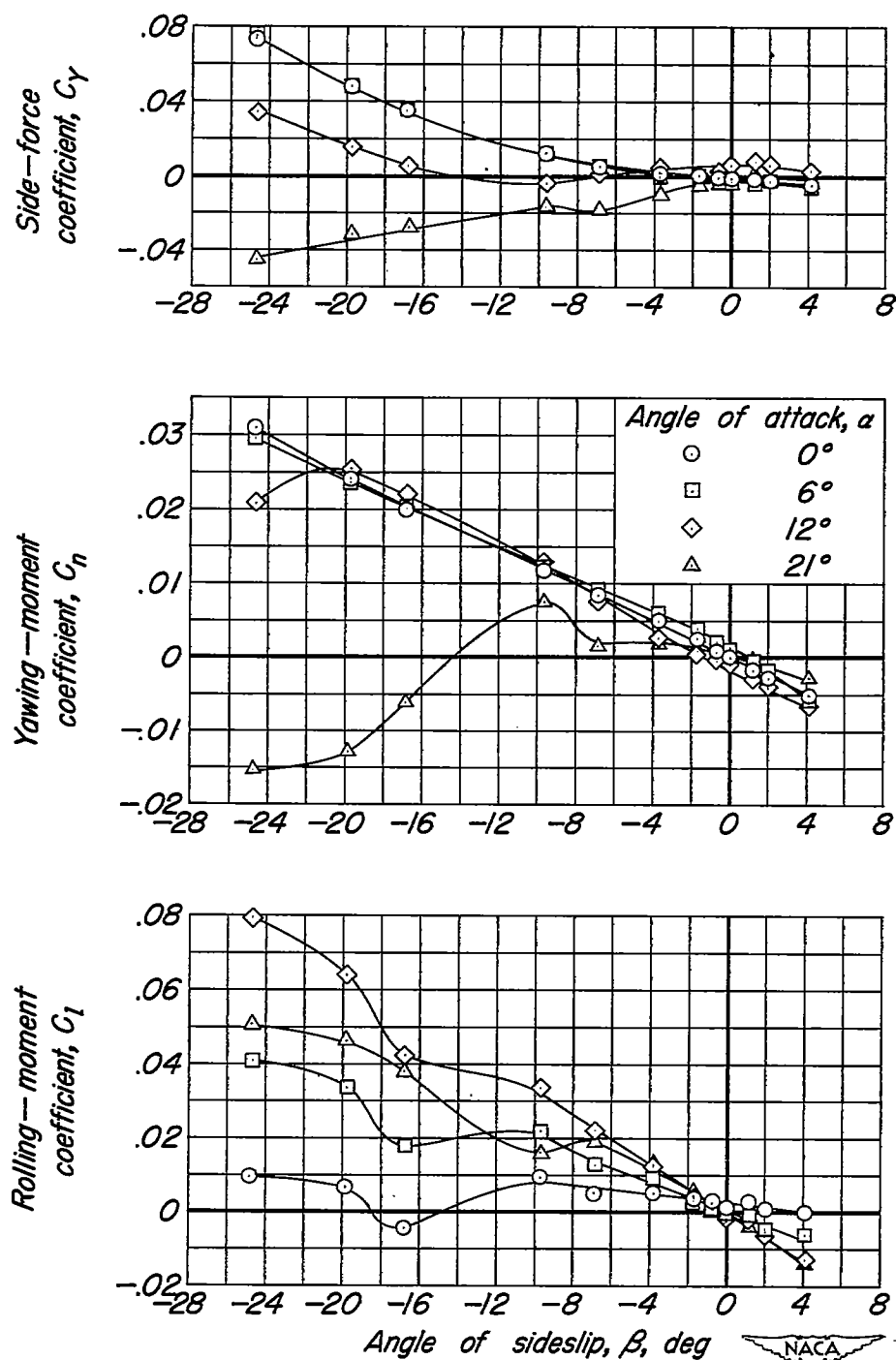
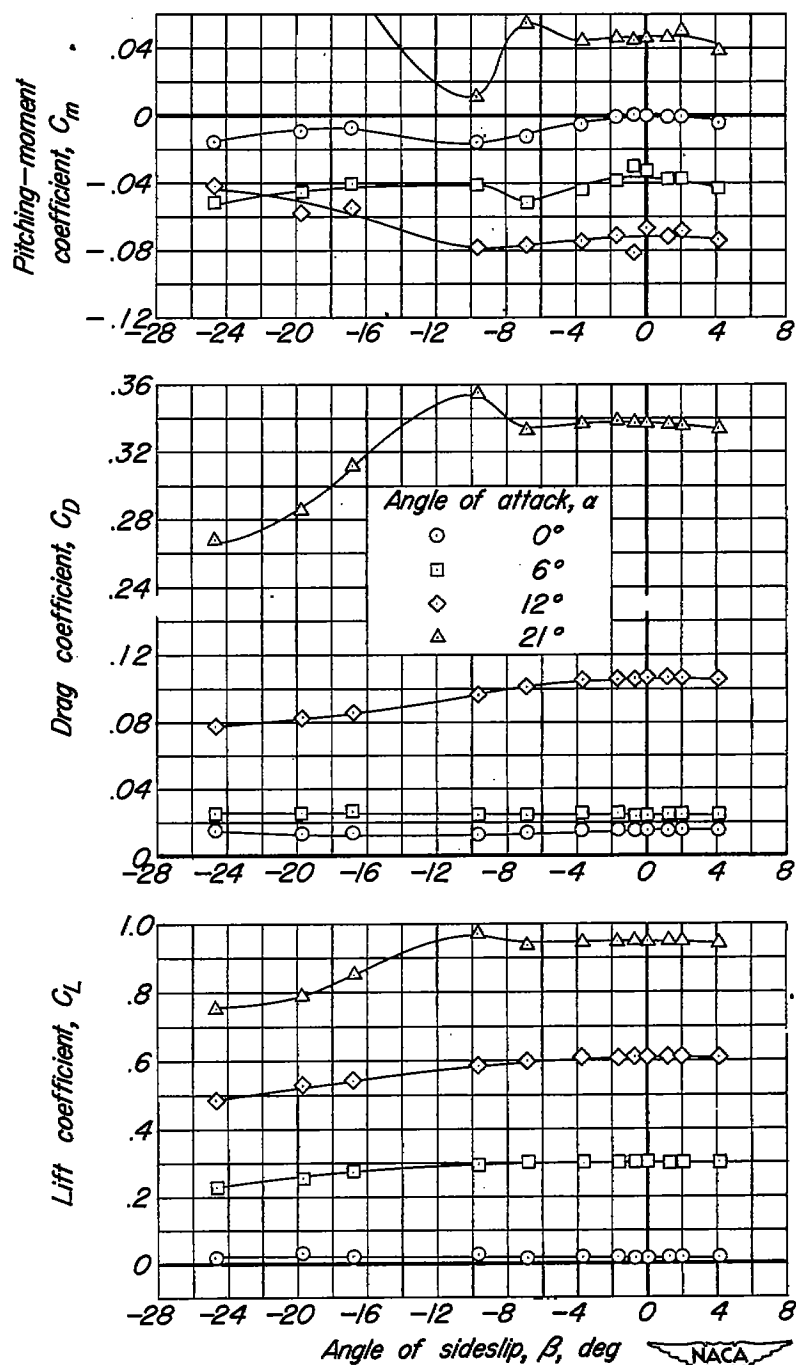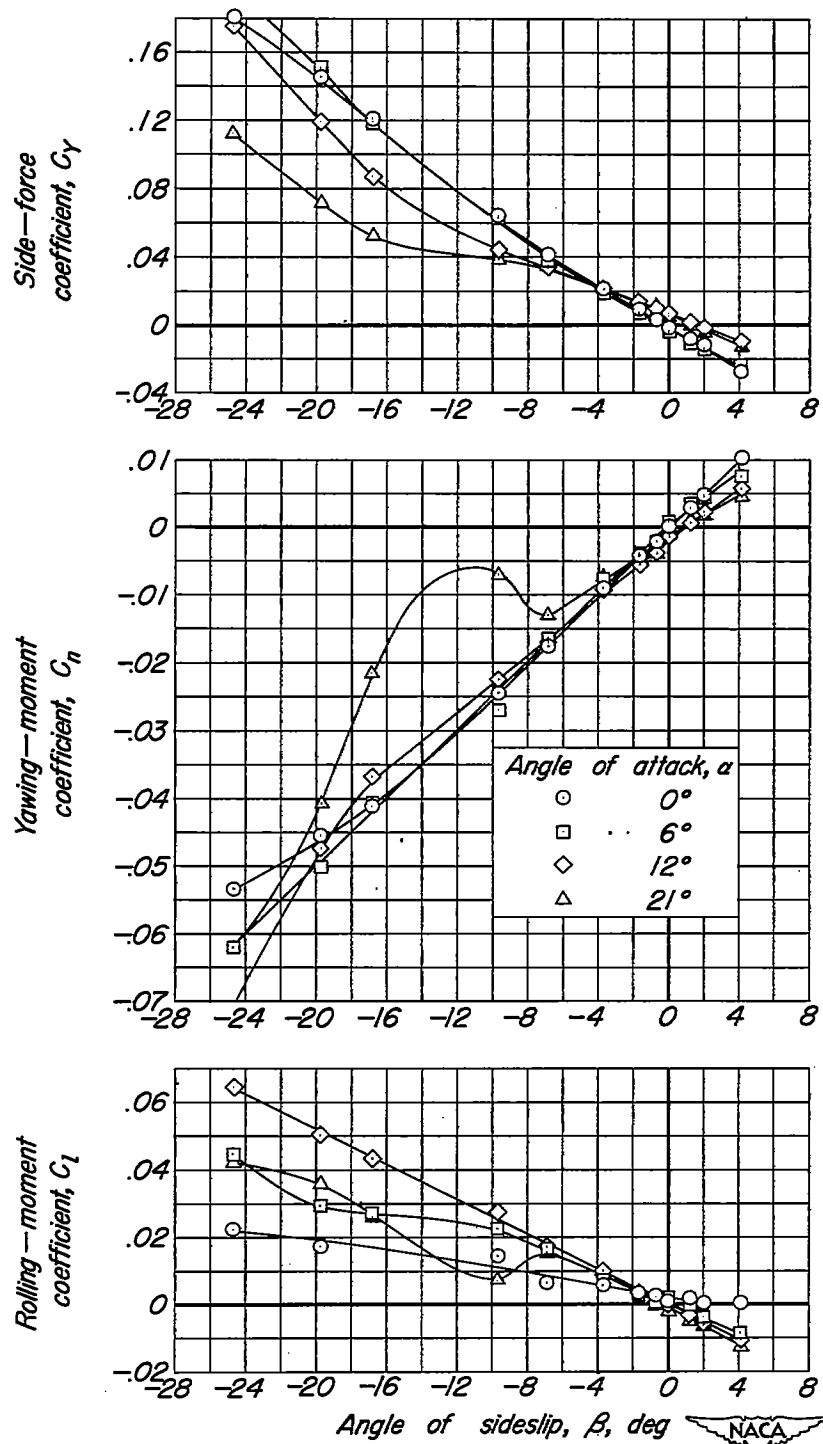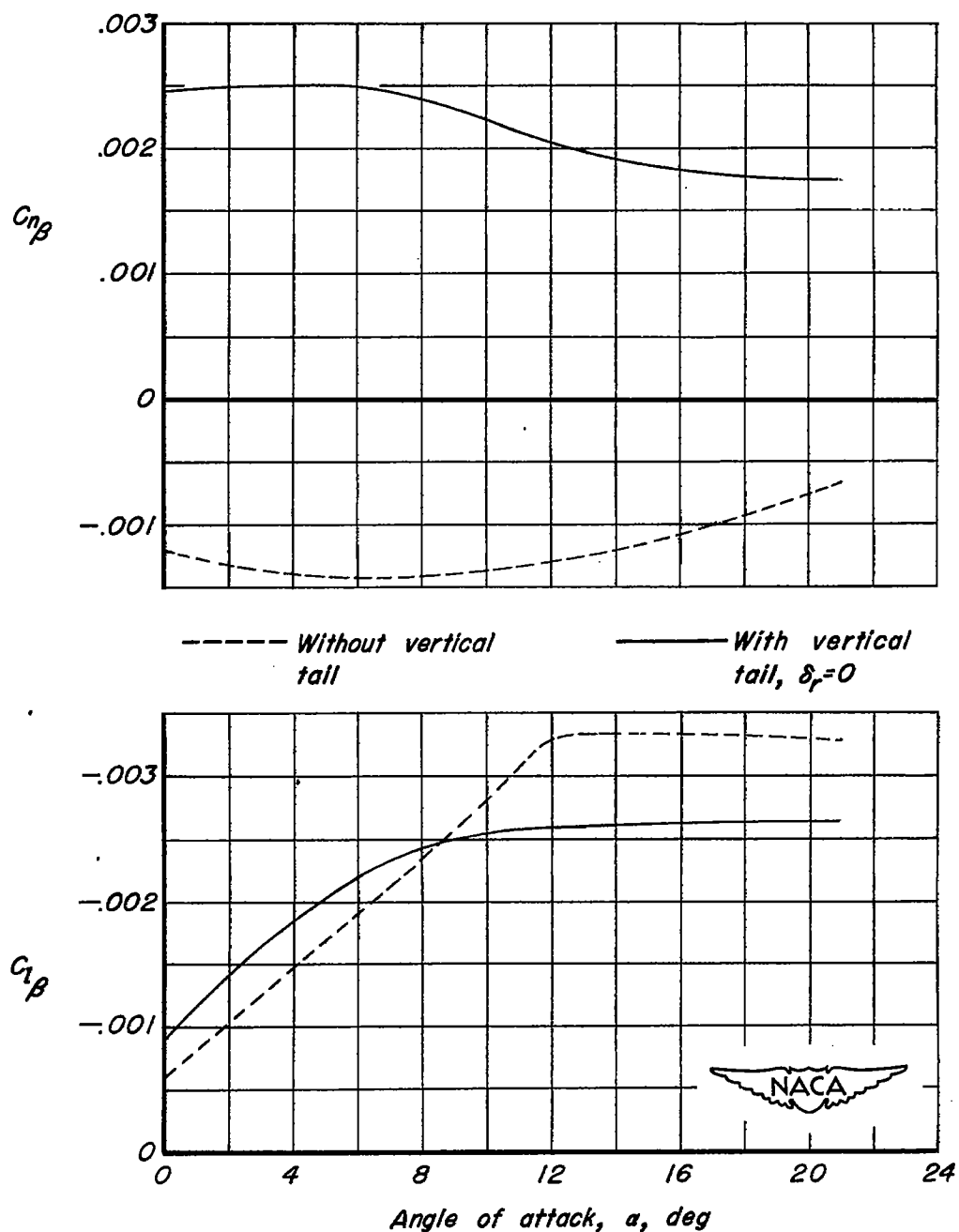(b) C_Y, C_n, C_l vs β.

Figure 4. — Concluded.

(a) C_m, C_D, C_L vs β.

Figure 5 . — Aerodynamic characteristics at several angles of attack of the 63° swept-back wing with fuselage. Vertical tail on.

Angle of attack, α

⊙ $0°$
□ $6°$
◇ $12°$
△ $21°$

Angle of sideslip, β, deg

(b) C_Y, C_n, C_l vs β.

Figure 5. — Concluded.

Figure 6.—Effect of the vertical tail on the values of the directional-stability parameter, C_{n_β}, and the effective-dihedral parameter, C_{l_β}, of the 63° swept-back wing with fuselage. $\beta = 0$.
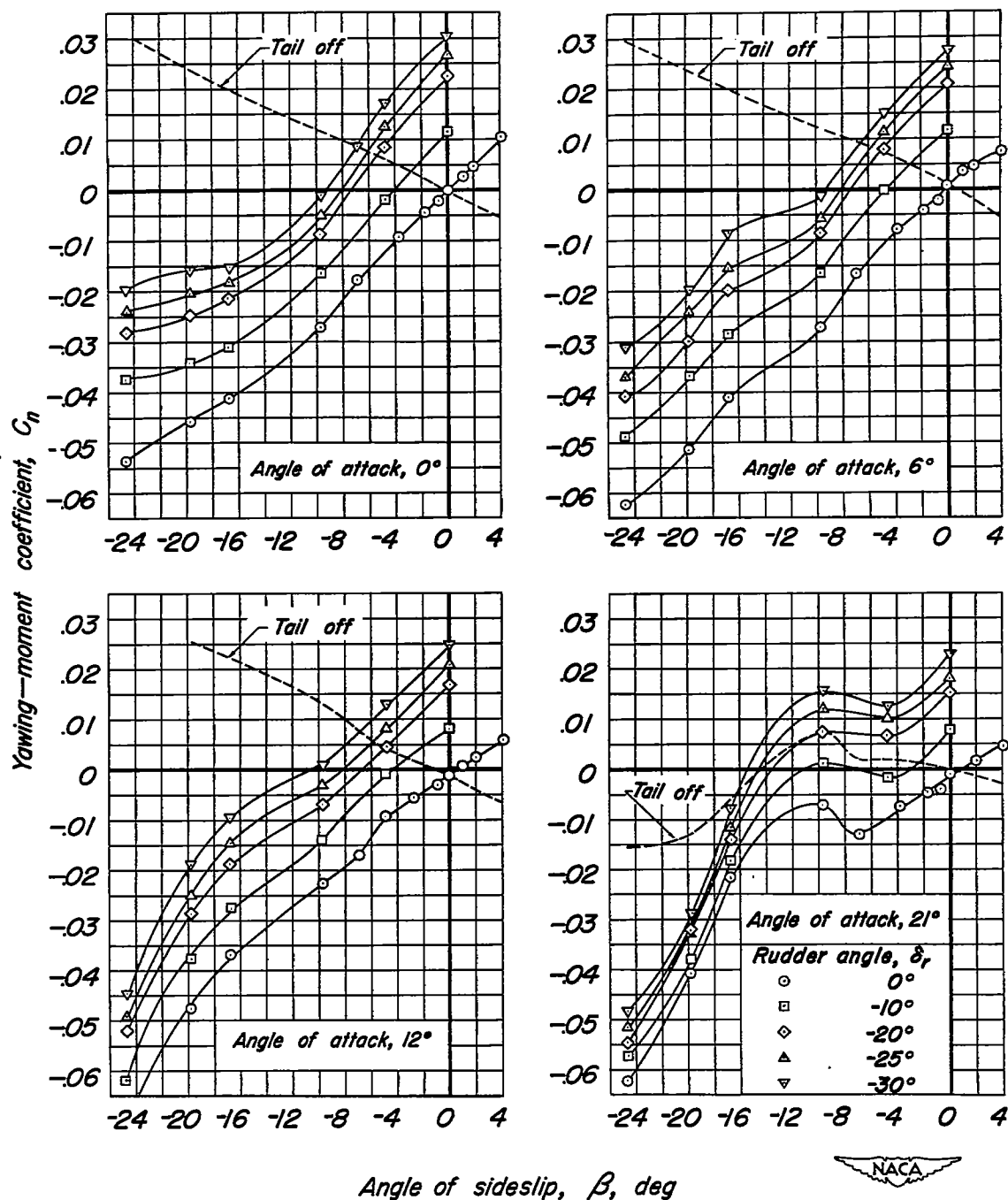
Figure 7. — Variation of yawing—moment coefficient with angle of sideslip for various rudder deflections. 63° swept-back wing—fuselage combination with vertical tail.
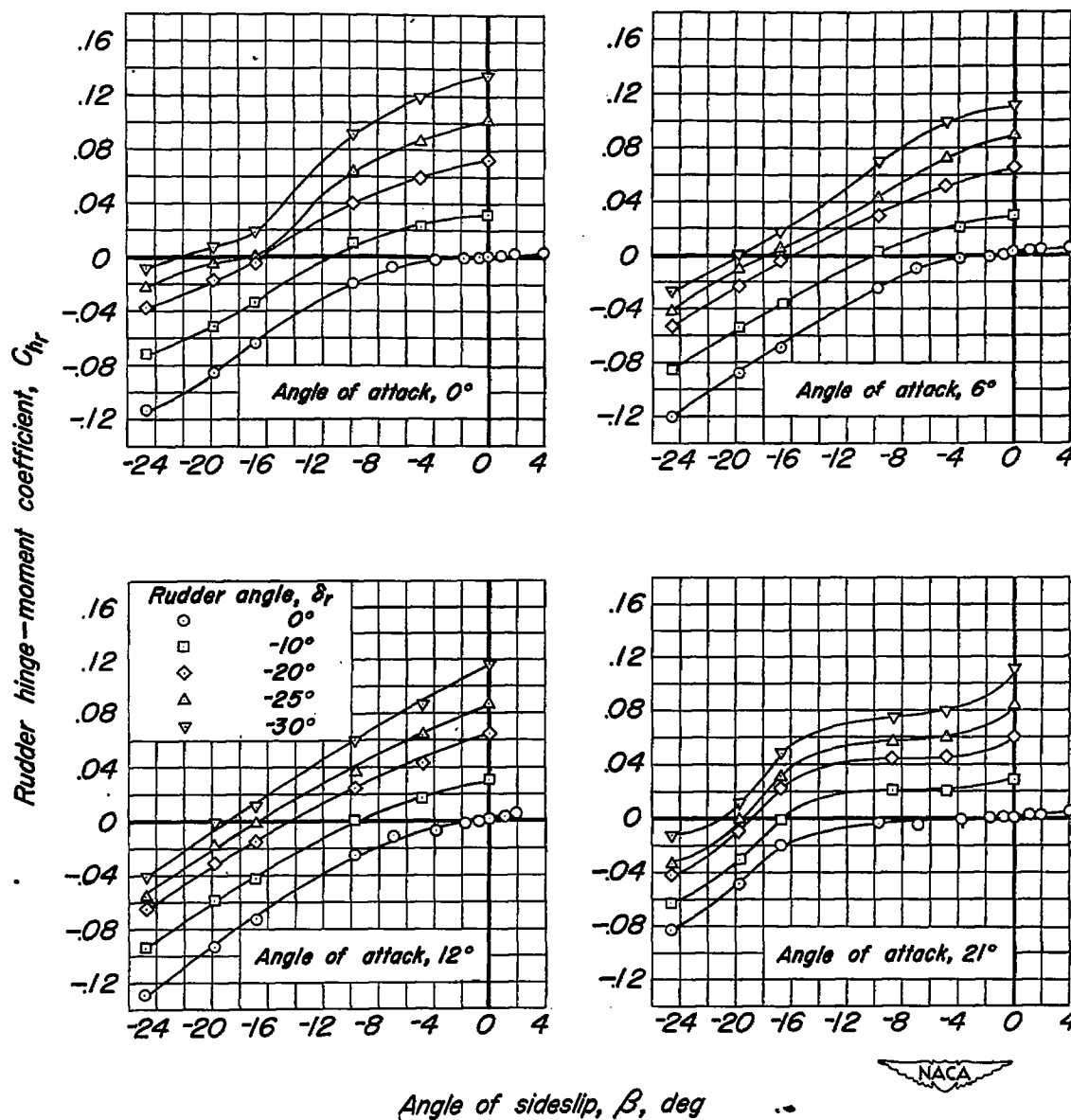
Figure 8. — Variation of rudder hinge—moment coefficient with angle of sideslip for various rudder deflections. 63° swept—back wing—fuselage combination with vertical tail.